Niobium for High Temperature Applications
Edited by Young-Won Kim and Tadeu Carneiro
TMS (The Minerals, Metals & Materials Society), 2004

DEVELOPMENT OF Re-BASED DIFFUSION BARRIER COATINGS ON Nb-BASED ALLOYS FOR HIGH TEMPERATURE APPLICATIONS

[1]Toshio Narita, [1-2]Michihisa Fukumoto, [1-1]Yuzi Matsumura, [1]Shigenari Hayashi, [2-1]Akio Kasama, [2]Isao Iwanaga, and [2]Ryohei Tanaka

[1]Research Group of Interface Control Engineering, Graduate School of Engineering,
Hokkaido University
Kita-13 Nishi-8, Kita-Ku, Sapporo 060-8628, Japan
Corresponding author e-mail address: narita@eng.hokudai.ac.jp
[1-1] A graduate student in Graduate School of Hokkaido University.
[1-2]A former graduate student in Graduate School of Hokkaido University and presently at Akita University
[2] Japan Ultra-high Temperature Materials Research Institute, Ube-city 507-0801, Japan
[2-1]presently at Kurume Technical College

Key words: Niobium alloy (based on Nb-5Mo-15W), Coatings, Diffusion barrier coating, High Temperature oxidation, Re-based alloys (based on σ phase of a Re-Cr-Ni system),

Abstract

Niobium based alloys are candidate materials for gas turbines that can be used, uncooled, at temperatures between 1473 and 1773K, while they suffer from severe degradation due to high temperature oxidation. In the present investigation to protect Nb-5Mo-15W alloy against high temperature oxidation a novel coating was developed with electroplating of a Re-Ni film, followed by Cr and Al pack cementation. The coating consisted of a duplex layer structure, an inner σ(Re-Cr) or Re(Cr) layer and an outer α Cr(Al) or β NiAl layer. The Re-Ni film containing more than 70at%Re, developed in the present investigation, is more useful than the conventional low Re-Ni film. The inner σ(Re-Cr) and Re(Cr) act as a diffusion barrier between the Nb-5Mo-15W alloy substrate and the outer σCr(Al) or β NiAl layer, which forms a protective α-Al_2O_3 scale. The Re-based alloy layers were considered to be an outer σ-phase in a Re-Cr(Ni) system and an inner χ-phase in a Re-Nb(Cr) system. The coated Nb-5Mo-15W alloy was oxidized in air at 1373 and 1473K for up to 360ks. It was found that due to a mutual reaction between the β-NiAl and the alloy substrate, the Re-based alloy layers with the σ-and χ-phases significantly suppressed the decomposition rate of the outermost β-NiAl in contrast to the rapid decomposition of conventional β-NiAl coatings without a diffusion barrier layer. The Re-based σ and χ phases are candidates for a diffusion barrier against Al inward diffusion, because they have very low solubility of Al. Diffusion couple studies shows that Nialuminides containing 12~50at%Al can be used as an Al-reservoir layer on the diffusion barrier layer of Re and Re-40Cr (σ Re_3Cr_2).

Introduction

Efficiency of turbine engines for both power generation and propulsion can be increased by raising the operating temperature of the engine. To attain these increased efficiencies, there is a need for high temperature materials that can be used, uncooled, at temperatures between 1473 and 1773K. Niobium based alloys (1) stand out compared to Ir-, W-, and Ta-based alloys because, as shown in Fig.1, they have the highest specific strength at temperatures above 1273K, where many Ni- and Co-based superalloys are approaching the upper limits of thermal durability (2–4).

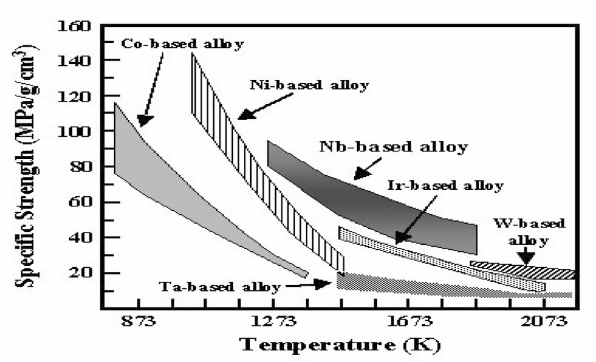

Fig.1 Temperature dependence of the specific strength of some high temperature alloy

Although Nb-based alloys are the most attractive for high temperature applications, they suffer from severe degradation due to high temperature oxidation. This may be in part due to the fact that Nb itself oxidizes rapidly, forming a non-protective oxide scale (5). Improvement of the oxidation resistance of Nb-based alloys is a key issue to the development of high performance gas turbines and to other high temperature applications.

A number of investigations(6–28) have been conducted with the aim to improve the high temperature oxidation resistance of Nb. These investigations include additions of alloying elements such as Cr, Al, Si, Ni, Mg, MgO and $MgSi_2$, and pack coatings by Cr and/or Al, slurry coating, and low pressure plasma spray overlay coatings. The formation of silicide coatings (20–28) on pure Nb and commercial Nb alloys was investigated extensively, with the coating conferring very good oxidation resistance at high temperatures. In particular, Rapp et al.(21) observed that tungsten and germanium-alloyed molybdenum disilicide coatings survived 1,800ks oxidation at 1643K with more than 100 thermal cycles.

Since water vapor is present in combustion environment, α materials of choice for this coating must be stable in water vapor at these elevated temperatures. Silica forming materials as silicon carbide and silicon nitride have been considered for structural applications in combustion environments; however, it was found that the thermal grown silica scale reacts with water vapor to form volatile hydroxides in combustion environments, precluding use for long-term applications (29).

Alumina is being considered to be more stable oxide than silica under combustion environments as a constituent of high temperature coatings (30). Recently, Opila et al. (31) assessed the stability of alumina in water vapor at elevated temperatures, reporting that alumina-based systems will have longer lifetimes than silica-based systems. In contrast to the disilicide coatings there are few reports dealing with a formation of a protective Al_2O_3 scale for elevated temperature applications. This may be in part due to the fact that the developed coatings appear to not perfectly cover the alloys, allowing easy access of oxidant gases such as oxygen and nitrogen through the coating. This leads to so-called under-cut corrosion, degrading the Nb-based alloy substrate beneath the coating.

It is widely accepted that both Al_2O_3 and SiO_2 forming coating deteriorate rapidly with increasing temperature due to both oxide formation and interdiffusion between the coating and alloy substrate, as shown schematically in Fig.2. Therefore, it is essential to suppress the interdiffusion in addition to ensuring slow oxide growth at very high temperatures. A coating with a two-layered structure, an inner diffusion barrier layer and an outer Al reservoir, is schematically shown in Fig. 3. The purpose of the diffusion barrier layer in Fig.3 is to reduce interdiffusion between the alloy substrate and the Al-reservoir layer, so that the barrier must have low diffusivity and low solubility of Al and alloying elements. For the Ni-based superalloys, the α-phase (32, 33, 34) in a Re-Cr-Ni system (35, 36) was selected as the diffusion barrier, because it has a high melting temperature of 2635K.

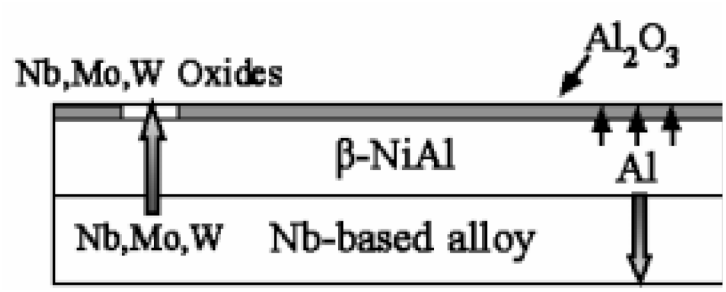

Fig.2
Schematic representation of the conventional β NiAl coating and its degradation due to mutual diffusion between the coating and alloy substrate.

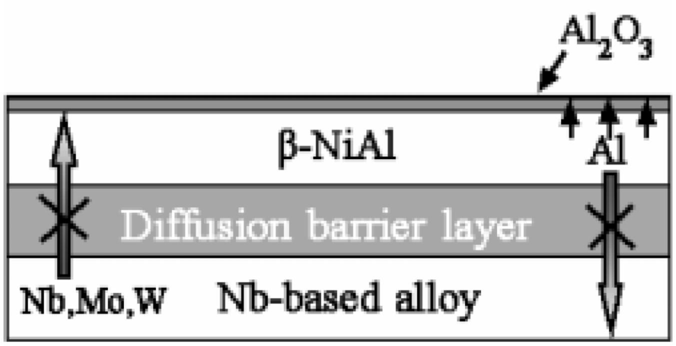

Fig.3
Schematic representation of the coatings with duplex layers of an inner, diffusion barrier and an outer, β-NiAl layer.

The formation process of the coating with a two-layered structure on the Nb-based alloy was investigated in previous studies (37, 38, 39), which used electroplating of a Re-Ni film as well as Cr and/or Al pack cementation. As described in a previous paper (39), a low Re-Ni film containing 25~35at%Re resulted in a non-protective coating and a high Re-Ni film containing 70at%Re or more showed the possibility of forming protective coatings. In that investigation, the high Re-Ni film was electroplated to form a coating with the two-layered structure on Nb-based alloys suggested in Fig.3, and the coating layer was evaluated to function an effective diffusion barrier. In this investigation a Nb-based alloy with an electroplated Ni film was used for the Al pack cementation, because conventional Al pack cementation forms non-protective coatings (10). The formation process and changes in the compositions of the two-layered structure are discussed based on the phase diagrams for the Re-Cr-Ni (35, 36), Re-Nb (40), and Nb-Al-Ni (41) systems.

To establish the diffusion coefficients of elements in a diffusion barrier layer of the Re-based alloy is essential and there must be compatibility among an Al-reservoir layer of for example nickel aluminides and a diffusion barrier layer. A series of investigation is now in progress in our laboratory to obtain information on the diffusion properties and compatibility between the σ-Re(Cr, Ni) and nickel aluminides. A diffusion couple study (42) between Re and Ni was carried out at temperatures between 1273 and 1573K using an Ar-arc melted Re and Ni as functions of composition and temperature as well as with a 7μ-φ Al_2O_3 marker fiber to determine intrinsic-diffusion coefficients at 1373K. It was found that two terminal solid solutions of Re(Ni) and Ni(Re) phases appeared in the diffusion couple, accompanied by the formation of voids in the Ni(Re) close to the Al_2O_3 marker position (about 3at%Re). It was concluded that Ni diffuses about 100 times faster than Re in the Re(Ni) and that this nonreciprocal diffusion may form voids within the Ni(Re) phase.

This paper investigates diffusion couples to elucidate details of diffusion between Re and nickel aluminides at high temperatures. The Ni-aluminides used are γ-Ni(12Al), γ-Ni_3Al, β-NiAl and δ-Ni_2Al_3, and couples of Ni-50Al and Re-Cr alloys or Re-Ni alloys were also investigated. A tentative Re-Ni-Al ternary phase diagram is developed using concentration profiles of each element measured across the diffusion couple composition paths.

Experimental

Nb-5%Mo-15%W alloy (mass%) was prepared in the Japan Ultra High Temperature Materials Research Institute (JUTEM) using non-consumable Ar arc melting with pure metals as starting materials. The alloy ingot was heat-treated in Ar at 2073K for 86.4ks. A 1 mm thick test specimen was cut from the ingot and then a 1.5mm diameter hole was drilled for suspension with a Pt-wire. The specimen was then degreased in a methanol/benzene solution under ultrasonic agitation.

The formation process of the two-layered coating was presented in elsewhere (39), so that the coating process with the high Re-Ni plating will be described briefly here.

1) The Nb-5Mo-15W alloy specimen was polished using 150-grit waterproof sand paper and then washed in a methanol/benzene solution.
2) A 10~15μm thick Re-Ni film containing more than 70at%Re of was electroplated from a pH=3 aqueous solution using a Ni anode at a bath temperature of 323K. The solution contains ReO_4 (0.1mol/l), nickel sulfate (0.1mol/l), and citric acid (0.1mol/l).
3) The Cr-pack cementation was carried out in a vacuum of 10^{-3}Pa at 1473K for 36ks using an Al_2O_3 crucible containing a specimen buried in a powder mixture of Ni-50Cr alloy and Al_2O_3.
4) A 10~15 μm thick Ni film was electroplated on the packed chromized alloy in the Watt's solution.
5) The Al-pack cementation was carried out at 1373K for 21.6ks in a vacuum of 10^{-3}Pa using an Al_2O_3 crucible containing the specimen and a powder mixture of fine Al particles, Fe-50Al alloy, and Al_2O_3.

The conventional Al-pack cementation was carried out as follows.

1) The Nb-5Mo-15W alloy specimen was polished using a 150-grit waterproof sand paper and then washed in a methanol/benzene solution.
2) A 10~15 μm thick Ni film was electroplated in the Watt's solution.
3) The Al-pack cementation was carried out at 1373K for 21.6ks in a vacuum of 10^{-3}Pa using an Al_2O_3 crucible containing a specimen in a powder mixture of fine Al particles, and Fe-50Al alloy, and Al_2O_3.

The coated specimens were oxidized in air for 90ks at 1373K or for 32.4ks at 1473K. The mass changes were measured using an electrical balance with an accuracy of 0.01mg. The coated and then oxidized specimens were examined using an electron-probe microanalyzer, EPMA, to determine the concentration of each element and their concentration profiles (compositions will be in at%, unless otherwise indicated); X-ray diffraction analysis XRD was used to identify oxidation products.

Results

3.1 Coating layer structures and concentration profiles

Figure 4 shows the microstructure and concentration profiles of each element across the about 12 μm thick Re-Ni film, which was electroplated from the pH=3 solution for 21.6ks under a current density 100A/m$_2$. The coating film composition is rather uniform 70Re-30Ni. There are cracks about every 20 μm that are parallel with the coating growth direction. These cracks may have formed when the sample was kept at room temperature after the electroplating. The gap at the film-alloy substrate interface ,ay have during metallurgical preparation.

A specimen with the Re-Ni film was then pack-chromized in a vacuum of 10^{-3}Pa at 1473K for 36ks, and a cross-sectional micrograph and corresponding concentration profiles of Re, Ni, Cr, Nb, Mo, and W across the specimen are shown in Fig. 5. It was found that the coating layer is comprised of a four-layer structure: an outer Cr-Re-Ni layer `5`, an inner Re-Cr-Nb layer `4`, a transient layer `3`, and a diffusion zone `2`, followed by the alloy substrate `1` (the circled numbers correspond to those in the figure being discussed). The diffusion zone contained Ni, which came from the Re-Ni film, but there was little Re or Cr; the outer and inner layers contained little of the alloy elements, Nb, Mo, and W, except for Nb in the inner layer. From the phase diagram of the Re-Cr-Ni system (35, 36) and also based on the compositions determined experimentally, the outer layer is the σ-phase in the Re-Cr-Ni system. Although details of the inner layer are not entirely clear because of a lack of an adequate phase diagram on the Re-Nb-Cr system, the inner layer seems to consist of the χ-phase in the Re-Nb system (40) . The identification of each phase will be discussed in a later section, but it is noted that further investigation is needed.

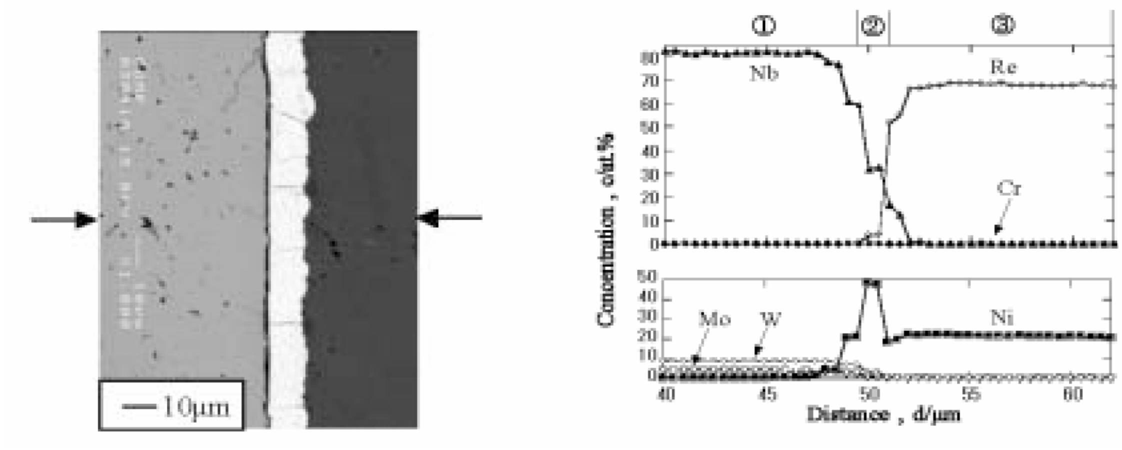

Fig.4 Cross sectional microstructure of the as-electroplated Re-Ni film on the Nb-5Mo-15W alloy and concentration profiles of the elements in the cross-section

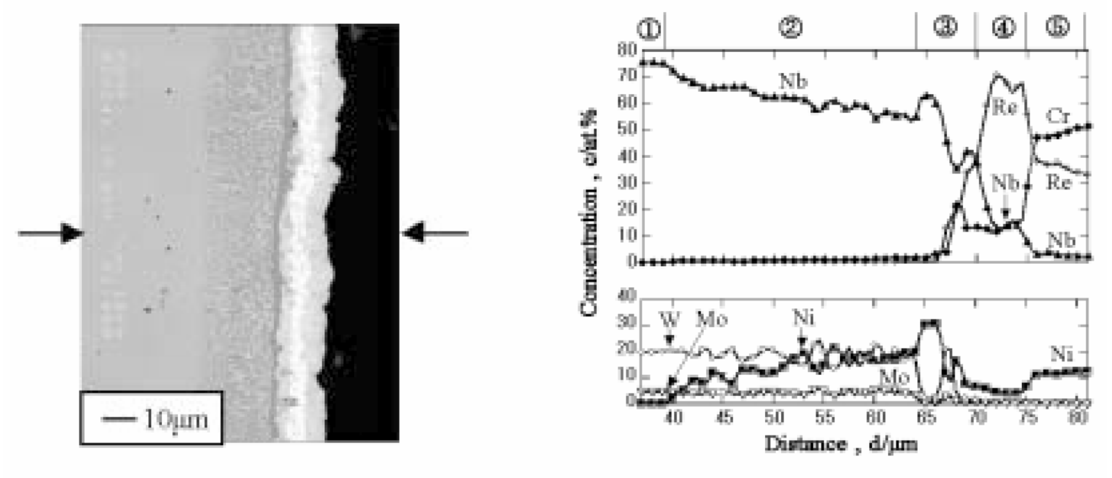

Fig.5 Cross-sectional microstructure and concentration profiles of the elements across the coating on theNb-5Mo-15W alloy after Cr-pack cementation at 1473K for 36ks. 1: alloy substrate; 2:diffusion zone ; 3:transient layer; 4:inner, χ-phase layer ; 5:outer, σ-phase layer.

After the Cr-pack cementation an about 10 μm Ni film was electroplated on the specimen, and then Al-pack cementation was carried out at 1373K for 21.6ks. Figure 6 shows the microstructure and concentration profiles of Re, Ni, Cr, Al, Nb, Mo, and W across the surface modified zone of the Nb-based alloy. The resulting coating is comprised of a four-layer structure: an outermost β-NiAl layer 5, an outer σ-phase layer 4, an inner χ-phase layer 3, and a diffusion zone 2.

The β-NiAl layer contains no Re, Cr, Nb, Mo, or W, and the oxygen is from the fine alumina particles embedded during the Al pack cementation. The layers 4, 3, and 2 contain little Al, and the Re content in the inner layer 3 is about 65at%. It may be concluded that the Re-based alloy layers act as a diffusion barrier against Al.

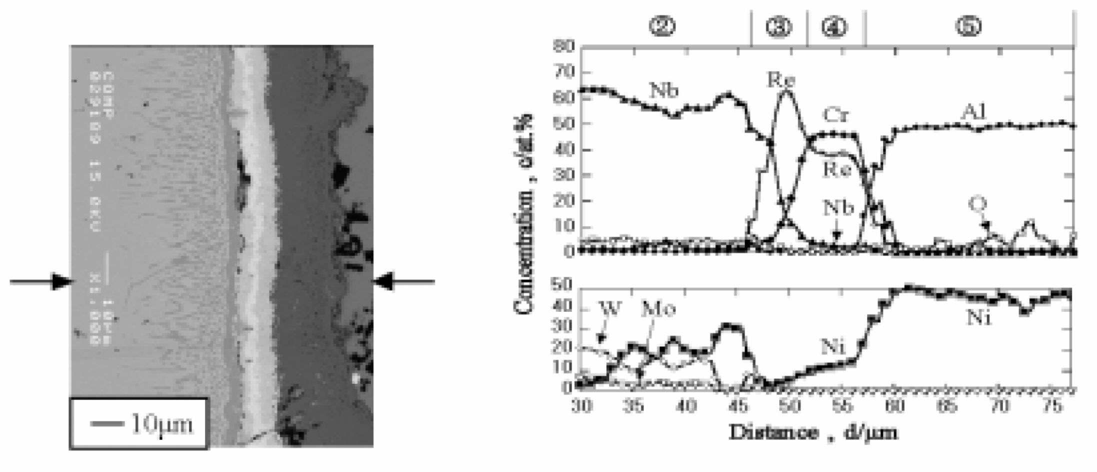

Fig.6 Cross-sectional microstructure and concentration profiles of the elements across the coating on theNb-5Mo-15W alloy after the Al-pack cementation at 1373K for 21.6ks. 2:diffusion zone; 3:inner χ-phase layer; 4:outer, σ-phase layer; 5: outermost, β-NiA

The Al-pack cementation was carried out for the Nb-based alloy with a pre-formed about 15 μm Ni at 1373K for 21.6ks, and the cross-sectional microstructure and corresponding concentration profiles of each element are shown in Fig. 7. The coating without the Re-based alloy layers consisted of a two-layered structure, an outer β-NiAl 4 and an inner diffusion zone (3+2). There were two distinguishable regions in the diffusion zone, one region 3 with both Al and Ni penetrations and another region 2 with Ni penetration. The outer β layer contains 50~52Al, with no alloying elements Nb, Mo, and W, and the oxygen in the outer layer is from fine Al_2O_3 particles, which were embedded during the Al pack cementation. Further, the oxygen in zone 3 may be the result of the fine Al_2O_3 particles that embedded in voids during the metallographic polishing process.

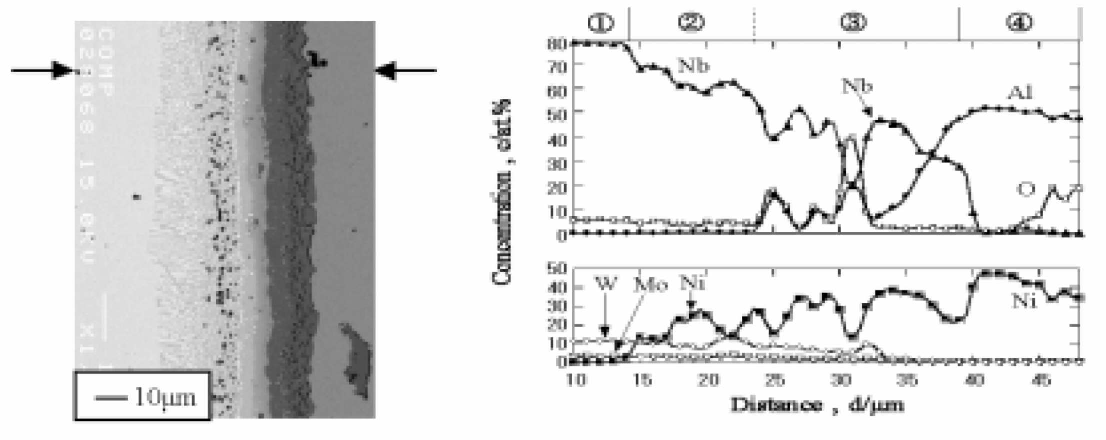

Fig.7 Cross-sectional microstructure and concentration profiles of the elements across the coating on theNb-5Mo-15W alloy after Al-pack cementation at 1373K for 21.6ks. 1 alloy substrate; 2 diffusion zone with Ni penetration; 3 diffusion zone with Al-and Ni-penetrations; 4 outer β-NiAl

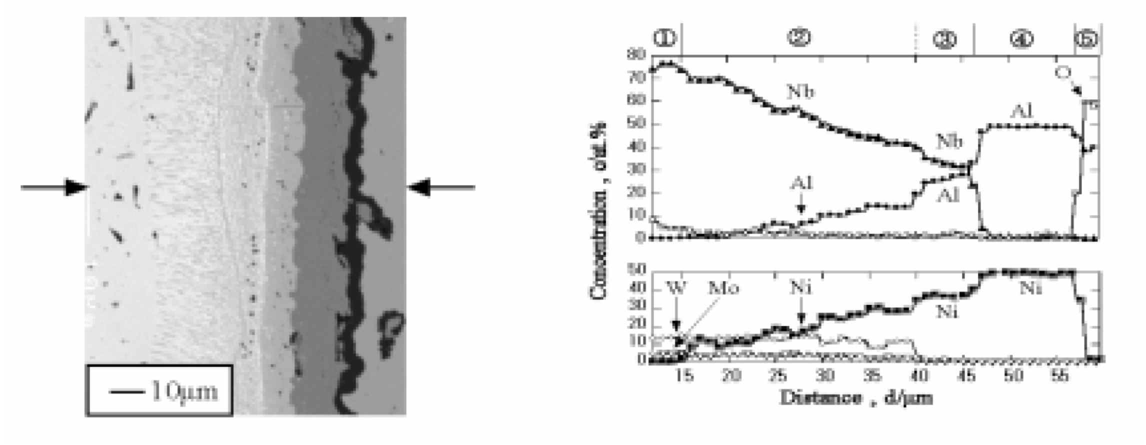

Fig.8 Cross-sectional microstructure and concentration profiles of the elements across the Al-pack coating on the Nb-5Mo-15W alloy after oxidation at 1373K for 90ks. 1 alloy substrate; 2 Al- and Ni-diffusion zone; 3 NbAlNi layer; 4 outer β-NiAl; 5 α-Al_2O_3 scale

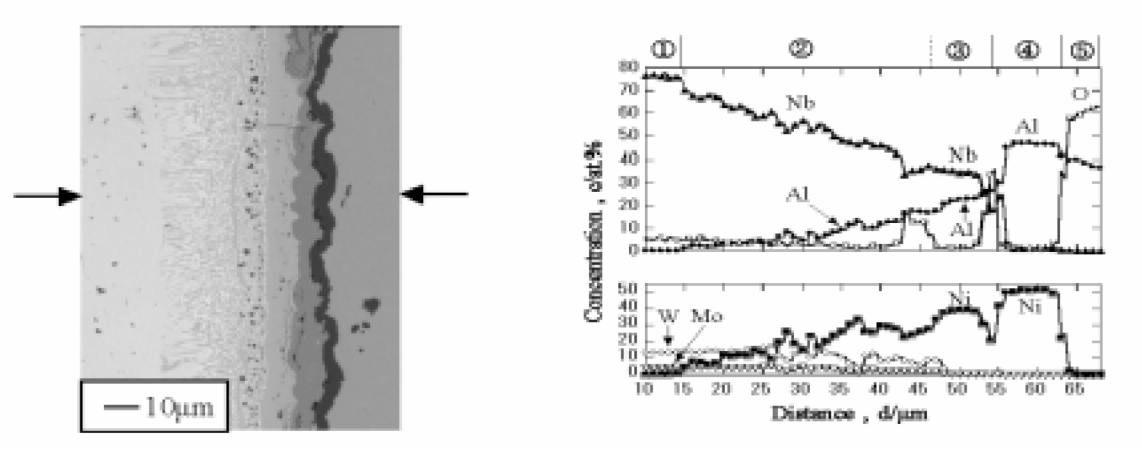

Fig.9 Cross-sectional microstructure and concentration profiles of the elements across the Al-pack coating on the Nb-5Mo-15W alloy after oxidation at 1473K for 32.4ks. 1 alloy substrate; 2 Al-and Ni-penetration zone; 3 NbAlNi layer; 4 outer β-NiAl 5 α-Al_2O_3 scale

3.2 Structures and concentration profiles of the Al pack / Ni film coating after oxidation

Figures 8 and 9 show the microstructure and concentration profiles of each element across the Al pack / Ni film coated Nb alloy (Fig. 7) after oxidation in air at 1373K for 90ks (Fig.8) and at 1473K for 32.4ks (Fig.9). In both specimens the coating layer consisted of a two-layer structure, an outer β-NiAl layer 4, which was covered by a protective Al_2O_3 scale 5, and a diffusion zone 2 and 3 with Al and Ni penetration. The diffusion zone was about 27 µm thick for the 1373K oxidation alloy, and 40 µm for the 1473K oxidation alloy.

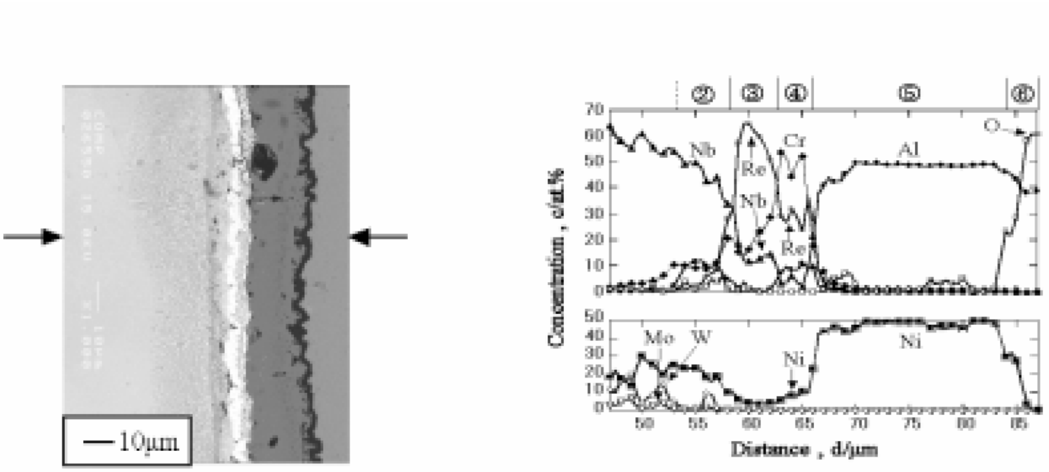

Fig.10 Cross-sectional microstructure and concentration profiles of the elements across the Re-based alloy coating on the Nb-5Mo-15W alloy after oxidation at 1373K for 90ks. 2 Al-penetration zone; 3 inner χ-phase layer; 4 outer, σ-phase layer; 5 outermost, β-NiAl; 6 α-Al_2O_3 scale

3.3 Structures and concentration profiles of the Re- based alloy / β-NiAl coating after oxidation

Figures 10 and 11 show the microstructure and concentration profiles of each element across the Re-based alloy / β-NiAl coated alloy (Fig. 6) after oxidation in air at 1373K for 90ks (Fig.10) and at 1473K for 32.4ks (Fig.11). The coating layer of both specimens consists of a four-layer structure, an outermost β-NiAl layer 5, which was covered by a protective Al_2O_3 scale 6 then an outer σ-phase layer 4, an inner χ-phase layer 3, and a diffusion zone 2 with Al penetration. The depth of the Al-penetration in the diffusion zone was about 5 μm in the alloy oxidized at 1373K and about 7 μm in the alloy oxidized at 1473K.

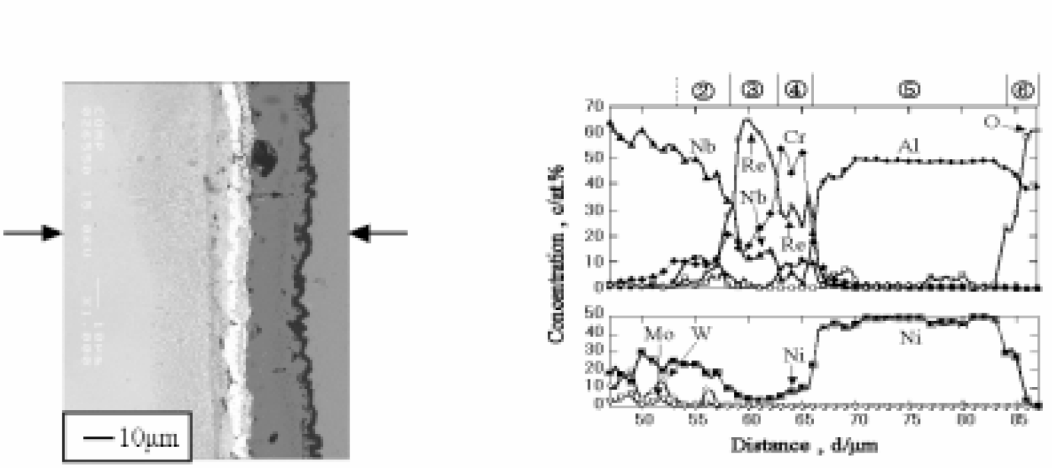

Fig.11 Cross-sectional microstructure and concentration profiles of the elements across the Re-based alloy coating on the Nb-5Mo-15W alloy after oxidation at 1473K for 32.4ks. 2 Al-penetration zone; 3 inner, χ-phase layer; 1 outer, σ phase layer; 5 outermost, β-NiAl;
6 α Al_2O_3 scale

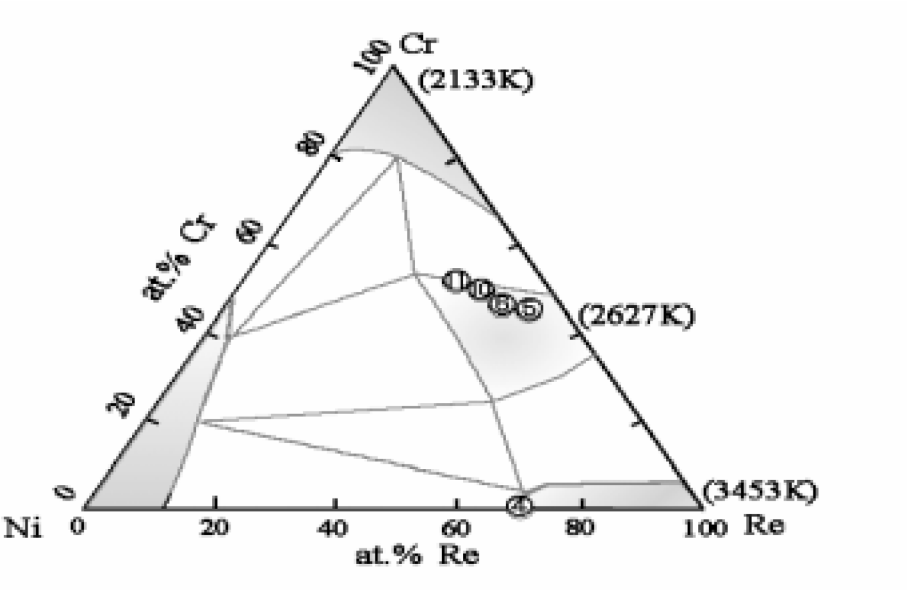

Fig.12 A phase diagram of a Re-Cr-Ni system at 1423K. 4 as-electroplated Re-Ni; 5 after the

Cr-pack cementation 6 after the Al pack cementation, 0 after oxidation at 1373K q after oxidation at 1473K

Discussion

The coating that developed on the Nb-5Mo-15W alloy in this investigation was a high-Re-Ni electroplated film, with Cr pack cementation then carried out to form a Re-based alloy layer. As shown in Fig. 5(a) and (b), the outer layer contained (47~52)Cr, (39~34)Re, (11~12)Ni and (1~3)Nb. From the phase diagram for the Re-Cr-Ni system calculated at 1423K (35, 36), the compositions in this outer layer 5 were inside the σ-phase. The inner layer 4 contained (64~72)Re, (25~13)Nb, (17~12)Cr, and (4~6)Ni and was inferred to be a χ-phase from the Nb-Re system (40). However, there is uncertainty in the identification of the inner layer phase, as a reliable phase diagram of the Re-Nb-Cr system is lacking. It is reasonable to assume it to be χ-phase from the Nb-Re system (40), as it exists adjacent to the Nb-based alloy, but further investigation to identify the phases is required.

For the coating layer in Fig. 6(a) and (b), the outer layer 4 contained 47Cr, (38~39)Re, (12~16)Ni, and a small amount of Nb. This composition is represented in Fig.12 by point , and it is seen to be close to those for the pack chromised specimen (Fig.5). It was found that the structure and concentration profiles of the Re-based alloy layers remain virtually the same before and after the Al pack cementation. Further, the layer 3 is a χ-phase with a composition of 18Cr, 15Nb, and 5Ni at a point with a 68Re in Fig.6, with the Al contents being negligible.

After oxidation at 1373K, as shown in Fig.10(b), the outer σ-phase layer has a composition of (46~52)Cr, (25~30)Re, (8~10)Ni, (8~10)Al, and a few % Nb, which is given by a number 0 in Fig.12, and the inner χ-phase layer 3 has 15Cr, 15Nb, 4Ni, and 68Re. Further, there are small amounts of Al in the inner layer 3. In the 1473K oxidation both the layers shown in Fig.11 have structures close to those for the 1373K oxidation. A composition of the layer 4 in Fig.11 is given by number q in Fig.12. From these results of oxidation at 1373 and 1473K it is concluded that there is little difference in the resulting structure and composition of the outer σ-phase and inner χ-phase Re-based alloy layers.

With the Al-pack / Ni film coating, the β-NiAl layer decomposed to a transient layer 3 with (38~33)Nb, 38Ni, and (24~28)Al, as a result of extensive Al penetration through the diffusion zone 2, as shown in Fig.8. The transient layer 3 in Fig.9 for the 1473K oxidation had a composition of (38~36)Nb, 40Ni, and (21~25)Al, due to Al penetration through the diffusion zone 2. The compositions in the transient layer 3 are indicated in the Nb-Al-Ni ternary phase diagram at 1413K in Fig.13, 8 for the 1373K oxidation and 8 for the 1473K oxidation, and both the transient layers appear to be an AlNbNi phase.

The β-NiAl phase in Fig. 13 contains about 7at%Nb, but there is little Nb in the coating layer before and after oxidation at both 1373 and 1473K, as shown in Figs. 8(b) and 9(b). Further investigation of the phase diagram of the Nb-Ni-Al ternary system at various temperatures is required to explain this conflict. The conventional Al packed coating (19) was severely degraded due to exfoliation of surface scale of niobium oxides in addition to Al_2O_3. Different from the conventional Al packed coating, the β-NiAl layer formed in the present investigation protects the Nb based alloy against high temperature oxidation, however, the protection may be limited to short term oxidation because rapid oxidation will commence when the β-NiAl layer is breached.

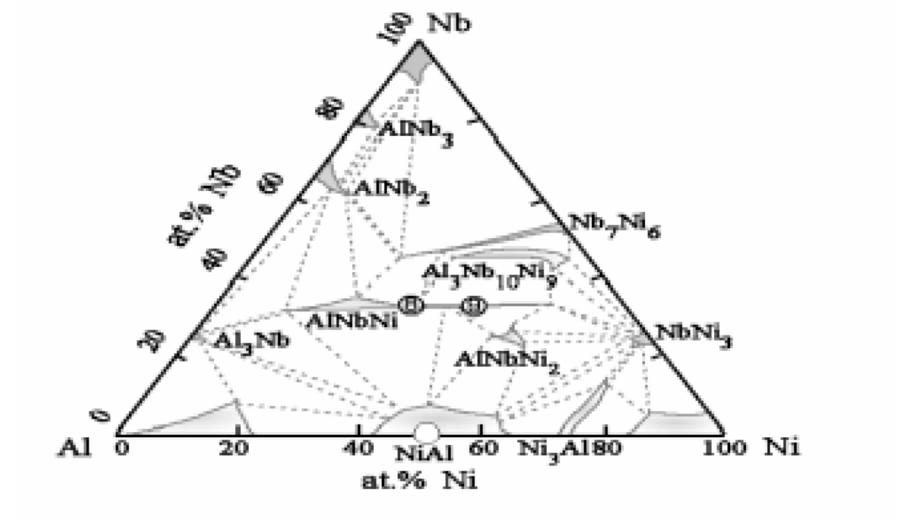

Fig.13 Phase diagram of the Nb-Ni-Al at1413K O: outermost β-NiAl layer. 8 after oxidation at 1373K 9 after oxidation at 1473K

The average thickness of the Al_2O_3 scale formed by the Al pack / Ni film coating are 2.6 μm after 90ks oxidation at 1373K and 4.5 μm after 32.4ks at 1473K and for the Re-based alloy / β-NiAl coatings 3.0 and 4.0 μm, respectively. This shows that the growth rates of the surface Al_2O_3 scale are similar, and that the changes in structure and concentration profile during oxidation are mainly due to mutual diffusion between the β-NiAl layer and alloy substrate. Therefore, it is concluded that the Re-based σ- and χ-phase layers developed in this investigation function as a diffusion barrier.

Figure 14 shows a phase diagram of a Re-Ni-Al ternary system at 1373K, which was hypothetically estimated from Re-Ni42), Ni-Al42), and Al-Re42) binary systems, because there is very limited information on the Re-Ni-Al ternary system in the literature41). In Fig.14 the solubility limit of Ni in Re was assumed to be about 28at%Ni from a previous investigation 43). The change in Al activity with Al contents in the Ni-Al binary system is also given in Fig.14.

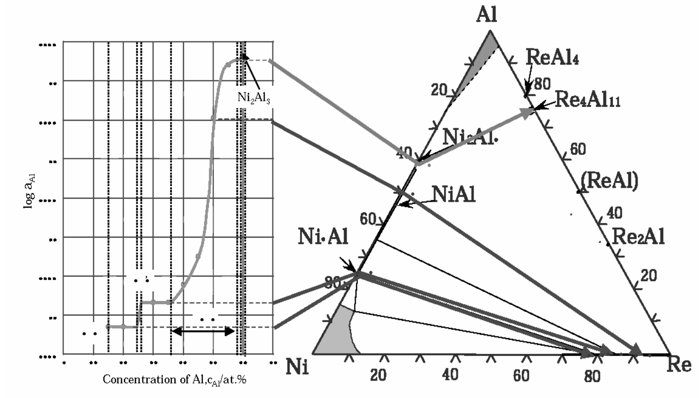

Fig.14
Composition paths for the Re and Ni aluminides couples plotted on the Re-Al-Ni ternary phase diagram and Al activities in the Ni-Al system as a function of Al contents.

From concentration profiles of Re, Ni, and Al for the Re and Ni-12Al(γ-Ni(Al)), the Re and Ni-25Al(γ-Ni_3Al), and the Re and Ni-50Al (β-NiAl) it was observed in these diffusion couples that Ni-aluminides were in contact with the Re and these was no formation of intermediate phases.

It was found that the Re contents in the Ni and the Ni aluminides tended to decrease from 12~13at%Re for the Re / Ni couple to 3~5at%Re in the Re / Ni-12Al (γ-Ni(Al)) couple and to be negligible for both the Re / Ni-25Al (γ^3-Ni_3Al) and the Re / Ni-50Al (β-NiAl) couples. The Ni contents in the Re decreased gradually from about 28at% for the Re / Ni couple to 20at%Ni for the Re / γ-Ni(Al), 15at%Ni for the Re / γ^3-Ni_3Al, and 10at%Ni for the Re / -NiAl.

In the case of the Re and Ni-60Al(δ-Ni_2Al_3,), however, the -Ni_2Al_3 reacted with the Re to form ReAl and Re_4Al_{11} accompanies by Al-rich β-NiAl transformed from the Ni_2Al_3, but no Re_2Al appeared. The concentration profiles of each element in the Re and Ni-60Al couple will be given by the composition path on the Re-Al-Ni phase diagram in Fig.14. It was found that the Re_4Al_{11} contains about 3at%Ni, while the Al-rich β-NiAl contains a little amounts of Re.

Conclusion

A Re-based alloy / β-NiAl coating was formed on Nb-5Mo-15W alloy and for comparison purposes Al pack / Ni film coating was also formed on the alloy. The coated alloys were oxidized in air at 1373K for 90ks and at 1473K for 32.4ks. The results obtained are summarized as follows.

1) The Re-based alloy/ β-NiAl coating was made in the following sequence: electroplating of a high Re-Ni alloy film, Cr pack cementation, Ni-film, and Al-pack cementation. The Re-based alloy layer consisted of an outer σ-phase layer and an inner χ-phase layer. The Nb-based alloy was pre-deposited with an electrolytic Ni film and the pack aluminized to form a β-NiAl layer accompanied by a diffusion zone allowing Al and Ni penetration.
2) The growth rates of the thermally grown Al_2O_3 scales were very similar on the coatings studied.
3) The β-NiAl layer without a Re-based alloy layer decomposed rapidly due to the mutual reaction between the NiAl and alloy substrate, accompanied by extensive penetration of Al into the alloy substrate.
4) With a Re-based alloy layer the β-NiAl layer remained in the coating, with the structure and concentration profiles remaining unchanged during high temperature exposure. The Al penetration was very slow.
5) The Re-based diffusion barrier layers have the following compositions:
   the as-prepared coating
      The outer layer:(46~52)Cr, (40~34)Re, 12Ni, (1~3)Nb
      The inner layer:(66~72)Re, 12Nb, (4~6)Ni, 1Cr
      after the 1373K oxidation
      The outer layer: (46~52)Cr, (40~34)Re, 12Ni
      The inner layer: (66~72)Re, 12Nb, (4~6)Ni, (1~3)Nb, 1Cr
      after the 1473K oxidation
      The outer layer: (46~52)Cr, (40~34)Re, 12Ni
      The inner layer: (66~72)Re, 12Nb, (4~6)Ni, (1~3)Nb, 1Cr
      There was little difference in composition of the outer σ-phase layer and the inner χ-phase layer before and after the oxidation tests. The phases were not finally identified.
6) The Al content in the χ-phase layer was negligible even after oxidation at 1473K for 32.4ks, and this is attributed to a slow Al penetration toward the alloy substrate.
7) On the Nb alloy, the coating with a β-NiAl layer formed by conventional Al pack cementation shows good oxidation resistance by forming a protective Al_2O_3 scale, but the protection is limited to short term oxidation.
8) Ni-aluminides containing 12~50at%Al can be used as an Al-reservoir layer on the diffusion barrier layer of Re and Re-40Cr (σ Re_3Cr_2).

Acknowledgement

The author is indebted to the New Energy and Industrial Technology Development Organization (NEDO) grant under contract number 11401050 (FY 2000 and 2001) supporting this investigation.

References

1) Y.Yamabe-Mitarai, Y. Ro, S. Nakazawa and H. Harada: J. Japan Inst. Metals, **64**(2000), 1068-1075.
2) C.L. Ma, A. Kasama, Y. Tan, H. Tanaka, R. Tanaka, Y. Mishima and S. Hanada: Report of the 123rd Committee on Heat-Resisting Materials and Alloys, Japan Society for the Promotion of Science, **40**(1999), 349-360.
3) R. Tanaka: MATERIALS AT HIGH TEMPERATURE, **17**(2001),457-464.
4) Y. Tan, H. Tanaka, C. Ma, A. Kasama, R. Tanaka, Y. Mishima and S. Hanada: J. Japan Inst. Metals, **64**(2000), 566-570.
5) OXIDATION OF METALS, ed. by K. Haufe, Plenum Press, pp.236-239 (1965).
6) J. A. Roberson and R. A. Rapp: Trans. Metallur. Soc. AIME, **239**(1965), 1327-1331.
7) D. W. Ayimore, S. J. Gregg and W. B. Jepson : J. Electrochem. Soc., **106**(1959), 1010-1013.
8) P. Kofstad and H. Kjollesdal; Trans. Metallur. Soc., AIME, **221,**(1961) 285-294.
9) M.G. Hebsur, J.R. Stephens, J.L. Smialek, C.A. Barrett, and D.S. Fox: Oxidation of High Temperature Intermetallics, ed. By T. Grobstein and J. Doychak, TMS, (1989), 171-184.
10) J. Doychak and M.G. Hebsur: Oxid. Met., **36**(1991),113-141.
11) H. J. Grabke, M. Steinhorst, M. Brumm, and D. Wiemer: Oxid. Met., **35** (1991), 199-222.
12)T. Hayashi and T. MaruyamaÅFJ. Japan Inst. Metals, **64** (2000), 1062-1067.
13) T. Murakami, S. Sasaki, K. Ichikawa, K. Adachi, K. Ito and M. Yamaguchi: Collected Abstracts of The 2000 Autumn Meeting of The Japan Inst. Metals, (2000), p. 438.
14) T. Murakami, K. Ito, M. Yamaguchi: Bulletin of Japan Inst. Metals (Materia Japan), **41**(2002), 432-439.
15) M. Matsubara and S. Hanada; J. Japan Inst. Metals, **63**(1999),112-117.
16) R.G. Weber, J. Bouvier and G. Slama; J. Less-Common Metals, **32**(1973), 1-20.
17) C.M. Packer: Oxidation of High Temperature Intermetallics, ed. By T. Grobstein and J. Doychak, TMS, (1989), 235-244.
18) T. Murakami, K. Ito, M. Yamaguchi, Bulleten of Japan Inst. Metals (Meteria Japan), **41** (2002), 432-439.
19) M.Fukumoto, Y.Matsumura, S.Hayashi, T.Narita, K.Sakamoto, A.kasama, and R.Tanaka; MATERIALS TRANSACTIONS of JIM, **44**(No.4)(2003), 731-735.
20) R. A. Perkins and G. H. Meier; Journal of Metals,**42**(1990), 17-21.
21) A. Mueller, G. Wang, R. R. Rapp, E. Courtright, and T. A. Kircher; Materials Science and Engineering A,**A-155**(1992), 199-207.
22) C.C.Wojcik; Mat. Res. Soc. Symp. Proc. 1994 MRS, **322**(1994) ,pp.519-530.
23) B.V. Cockeram, H.J.Schmutzler, J. Shyue, K. Hoshino, S.Meng, R. Wheeler, and H.L.Fraser; Mat. Res. Sco. Symp. 1995 MRS,**364**(1995), pp.1327-1332
24) M. Vilasi, H.Brequel, R. Podor and J.Steinmetz; “Elevated Temperature Coatings: Science and Technology Ö†, editedby N.B.Dahotre and J.M.Hampton, The Minerals, metals and Materials Society, (1996) 233-242.
25) M. Vilasi, M. Francois, R.Podor and J.Steinmetze; Journal of Alloys and Compounds, **264**(1998), 244-251.
26) Y. Li, W. Soboyejo, and R.A. Rapp, Metallurgical and Materials Transactions

B,**30**(1999) 495-504.

27) Y. Wang, J.Gao, Y.Li, and X.Hu;Journal of Inorganic Materials (Chinese),**15**(2000), 143-149.

28) R. O.Suzuki, M.Ishikawa, and K. Ono; Journal of Alloys and Compounds,**336**(2002), 280-285.

29) I.Yuri and T.Hisamatsu: ASME Turbo Expo, paper GT2003-38886.

30) R.Gadow and M.Lischka: Surface and Coating Technology, 151-152(2002), 392-399.

31) E.J.Opila and D.L.Myers: Proceedings of the Symposium on High Temperature Corrosion and Materials Chemistry, IV , Electrochemical Society, held April 28- May 5, 2003 in Paris.

32) T. Narita, Y. Hisamatsu, M. Shoji, and S. Hayashi: Report of the 123rd Committee on Heat-Resisting Materials and Alloys, Japan Society for the Promotion of Science, **41**(2000), 127-134.

33) T. Narita, M. Shoji, Y. Hisamatsu, D. Yoshida, M. Fukumoto, and S. Hayashi: MATERIALS AT HIGH TEMPERATURES, **18**(2001), 245-252.

34) T. Narita, S. Hayashi, M. Shoji, Y. Hisamatsu, D. Yoshida, and M. Fukumoto: CORROSION 2001 NACE International, Houston Texas, (2001), paper 01157.

35) C. M. Neubauer, D. Mari and D.C. Dunabd; Scripta Metallurgica et Materilia; **31**(1994), 99-104.

36) W. Huang, Y.A.Chang; J. Alloys and Compounds, **274**(1998), 209-216.

37) M. Fukumoto, Y. Matsumura, S, Hayashi, T, Narita, K. Sakamoto, A. Kasama, R. Tanaka; Report of the 123rd Committee on Heat-Resisting Materials and Alloys, Japan Society for the Promotion of Science, **43**(2002), 383-390.

38) M. Fukumoto, Y. Matsumura, S, Hayashi, T, Narita, K. Sakamoto, A. Kasama, R. Tanaka; submitted to Materials Transaction of JIM.

39) M. Fukumoto, Y. Matsumura, S, Hayashi, T, Narita, K. Sakamoto, A. Kasama, R. Tanaka; submitted to Oxid. Met.

40) Desk Handbook Phase Diagrams for Binary Alloys, edited by H. Okamoto, ASM, (2000), p.599.

41) Handbook of Ternary Alloy Phase Diagrams, edited by P. Villars, A. Prince and H. Okamoto ASM International, Vol.4 (1995), p.4124.

42)Phase diagrams for Binary Alloys, edited by H.Okamoto, ASM International (2000), p.619 for a Ni-Re system, p.38 for an Al-Ni system and p.41 for an Al-Re system.

43) S. Narita, Master thesis, (Hokkaido University,